Journal of Pharmaceutical and Biomedical Analysis 252 (2025) 116480

Contents lists available at ScienceDirect

Journal of Pharmaceutical and Biomedical Analysis

journal homepage: www.journals.elsevier.com/journal-of-pharmaceutical-and-biomedical-analysis

Short communication

Derivatization to reduce background interferences for simultaneous quantitation of trimethylamine (TMA) and trimethylamine-*N*-oxide (TMAO) using liquid chromatography with tandem mass spectrometry

Maria A. Valdivia-Garcia, Yang Bi, Kaoutar Abaakil, Jia V Li *

Section of Nutrition, Division of Digestive Diseases, Department of Metabolism, Digestion and Reproduction, Faculty of Medicine, Imperial College London, Hammersmith Campus, Commonwealth Building, Du Cane Road, London W12 0NN, United Kingdom

ARTICLE INFO

Keywords:
Derivatisation
UPLC-MS/MS
Ethyl bromoacetate
Sodium heptanesulfonate

ABSTRACT

Trimethylamine (TMA) and trimethylamine-*N*-oxide (TMAO) play a crucial role in many biochemical processes within diverse organisms including animals, plants, fungi and bacteria. Studies have linked these metabolites with cardiovascular and kidney diseases; however, emerging evidence demonstrates their protective properties. Owing to these controversies and co-existence of these metabolites in biological samples, it is crucial to accurately quantify these metabolites to associate their concentrations with various physiological and pathophysiological conditions to elucidate their potential roles. We reported interferences on TMA quantification without derivatizing the analyte. A combined sample preparation method, including sample derivatization with ethyl bromoacetate and use of ion pairing reagent (sodium heptanesulfonate), minimized these interferences and provided improved accuracy and precision for simultaneous quantification of TMA and TMAO. The linearity for TMAO ranged from 0.01 μM to 300 μM and 0.1 μM - 300 μM for TMA. With the application of this method, we reported that the circulating concentrations of TMA was 4 times higher in male mice (33.1 ± 5.9 μmol/L) compared to females (8.3 ± 1.39 μmol/L), whereas TMAO levels were 6 times lower in male (7.2 ± 0.4 μmol/L) than female mice (42.1 ± 4.5 μmol/L). In contrast, concentrations of TMA and TMAO in the colonic tissue did not differ significantly between males and females. The robust analytical method for simultaneously quantifying TMA and TMAO presents a significant value in facilitating investigations on TMA and TMAO biology.

1. Introduction

Trimethylamine (TMA) is produced by the gut bacteria from the dietary quaternary amines such as choline, betaine and carnitine. It is volatile (boiling point at 2.9°C) and has a distinctive odour associated to rotting fish [1]. In the liver of higher vertebrates, TMA is oxidized by flavin-monooxygenase 3 (FMO3) to trimethylamine-*N*-oxide (TMAO) [1]. High blood levels of TMAO have been associated with cardiovascular risk [2] and kidney damage [3]; however, TMAO has also been shown to alleviate H_2O_2-induced oxidative stress damage of cells [4]. Owing to their important biological implications, it is crucial to quantitate these metabolites in various biofluids and tissues, enabling the evaluation of impact of diet and the gut microbiota on TMA and TMAO concentrations.

Several studies have reported qualitative and quantitative measurement of TMAO and TMA using diverse techniques including nuclear magnetic resonance (NMR) spectroscopy [1,5], and gas and liquid chromatographic separations coupled with tandem or high resolution mass spectrometry (MS) [6,7]. Owing to the sensitivity limitation of NMR spectroscopy, it is not ideal for quantifying TMA and TMAO in tissue samples, in which their concentrations are low. Gas chromatography coupled with MS (GC-MS) was successfully used to measure these compounds [6,8], but the process was lengthy as it applied several extraction and derivatisation steps. On the other hand, hydrophilic interaction liquid chromatography coupled with tandem MS (HILIC-MS/MS) facilitates a better separation of TMA and TMAO and improves the detection by enabling the selection of specific masses [9,10]. Measured concentrations of TMA in plasma from healthy subjects differ considerably from one study to another (Table 1). Furthermore, some methodological details and crucial mass spectrometer specification, such as *m/z* detection ranges at the given acquisition rates, are lacking in literature, which hinders the method implementation in other

* Corresponding author.
E-mail address: jia.li@imperial.ac.uk (J. V Li).

https://doi.org/10.1016/j.jpba.2024.116480
Received 29 July 2024; Received in revised form 6 September 2024; Accepted 16 September 2024
Available online 20 September 2024

Table 1
Reported concentrations of TMA in different biological samples using GC-MS and LC-MS/MS.

Authors	LC Separation	Masses $[M+H]^+$	Internal standard/ Derivatisation	Platform	TMA average concentrations (controls)	Organism	Tissue
Awwad, et al [10].	BEH-HILIC	60,44	TMA-d_9/N.A	LC-MS/MS	0.86 µmol/L	Human	Plasma
Zordoky, et al [12].	Biocrates-RP	59	N.A/N.A	LC-MS/MS	26.55 (unit not reported)	Human	Plasma
Bain, et al [13].	SPME	58, 66	TMA-d_9/N.A	GC-MS/ MS	0.418 µmol/L	Human	Plasma
Hefni, et al [9].	HILIC-N	146, 117, 99	TMA-d_9/EBA, IAM, IACN	LC-MS/MS	0.98 µmol/L	Human	Plasma
Hefni, et al [9].	HILIC-N	146, 117, 99	TMA-d_9/EBA, IAM, IACN	LC-MS/MS	4.4 µmol/L	Human	Urine
Johnson, et al [14].	Direct infusion	146.1, 118.1	TMA-d_9/EBA	LC-MS/MS	0.11–1.19 mmol/mol creatinine	Human	Urine
Awwad, et al [10].	BEH-HILIC	60,44	TMA-d_9/N.A	LC-MS/MS	3.4 µmol/L	Human	Urine
Roggensack, et al [15].	BEH-HILIC	60,44	TMA-d_9/N.A	LC-MS/MS	n.d	Human	
Veeravalli, et al [16].	ACE® C18 RP	146	TMA-d_9/EBA	LC-MS/MS	0.07–3.09 mM/Creatinine(mM)	Mouse	Urine
Hoyles, et al [17].	BEH-HILIC	146,118, 150, 122	TMA-d_9, $^{13}C_3$/^{15}N-TMA, EBA	LC-MS/MS	12.5 µmol/L	Mouse	Plasma
Cai, et al [18].	BEH-HILIC	60,44	N.A/N.A	LC-MS/MS	Relative Abundance	Bacteria	

n.d: non-detectable
RP: Reverse phase; EBA: Ethyl bromoacetate; IACN: Iodo-acetonitrile; IAM: Iodo-acetonitrile-acetamide
HILIC-N: Hydrophilic interaction liquid chromatography neutral
SPME: Solid Phase Micro Extraction
ACE® C18 RP: Advanced Chromatography Technologies Trademark, eighteen carbon
BEH: Bridged ethylene particle
N.A: Non-available

laboratories. In our study, we aimed to develop a simple method to address these limitations in simultaneously quantitating TMA and TMAO using LC-MS/MS.

2. Materials and methods

2.1. Biofluid and tissue sample collection

Seventeen female and 16 male Fabpl *Cre* ;*Apc*$^{15lox/+}$ [11] mice were bred and maintained under standard conditions (room temperature at 21 ± 1°C; 12-h light-dark cycle) and provided *ad libitum* with normal chow diet and water throughout the experiment. Mice were

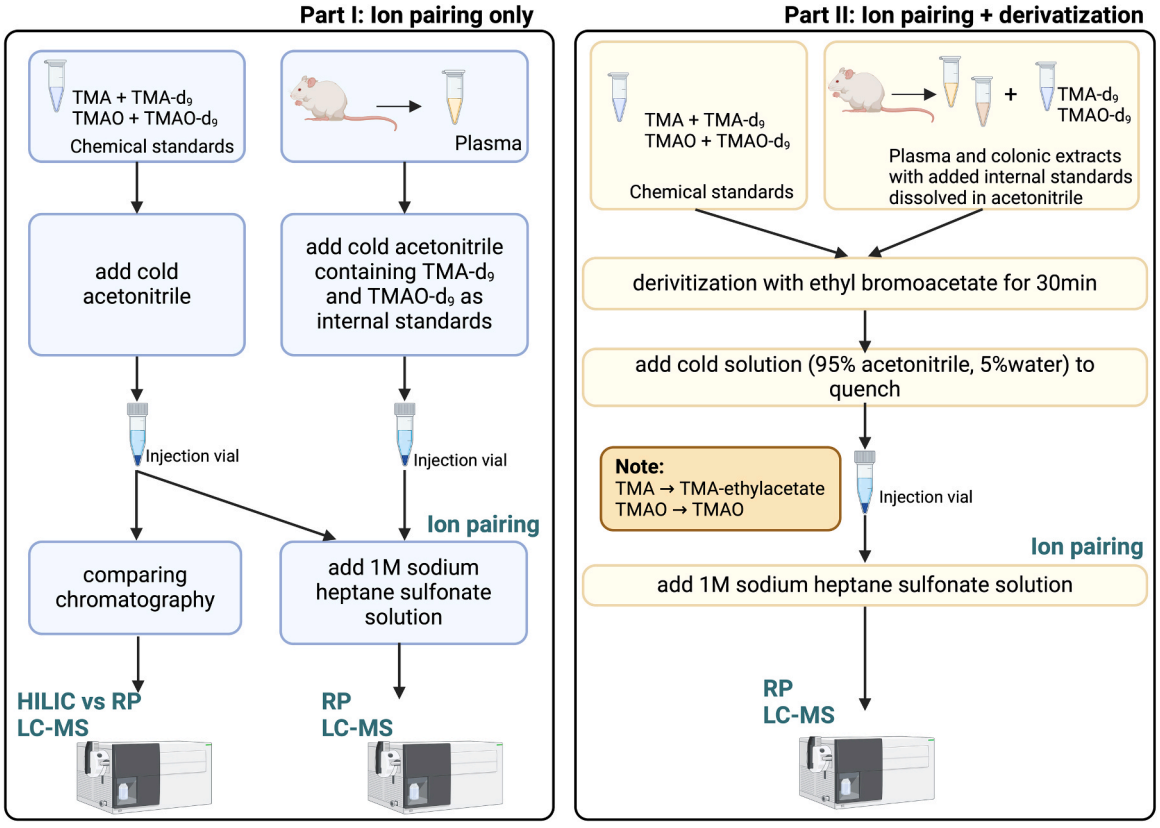

Fig. 1. A flowchart of the method development involving ion pairing alone or the combined method of derivatization and ion pairing. Created in BioRender. Abaakil, K. (2024) BioRender.com/y22y390.

Table 2
Multiple Reaction Monitoring (MRM) Parameters.

Compound	Segment time (min)	Retention Time (min)	Precursor ions	Product ions	Cone voltage (V)	Collision energy (V)	Dwell time (s)
TMAO	2.2–3.0	2.51	76.1	58.1	5	10	0.02
	2.2–3.0	2.51	76.1	59.1	5	10	0.02
	2.2–3.0	2.51	76.1	76.1	5	10	0.02
TMAO-d_9	2.2–3.0	2.50	85.0	66.0	5	10	0.02
	2.2–3.0	2.50	85.0	68.0	5	10	0.02
TMA-ethyl-acetate	2.2–3.0	2.70	146.1	118.1	10	5	0.02
TMA-d_9-ethyl-acetate	2.2–3.0	2.70	155.1	127.1	10	5	0.02

sacrificed at age of 13 weeks for male and 15 weeks for female. Tissue samples were collected, immediately frozen in liquid nitrogen and stored at −80°C until further analysis. Animal experiments were carried out under a Home Office project licence (PPL P9718F9C8). The blood was collected into heparin-coated capillary tubes using tail venipuncture, centrifuged at 11,200*g* for 3 min to obtain plasma. Colonic tissues were collected and snap-frozen in liquid nitrogen. Both plasma and colonic tissues were subsequently stored at −80°C pending for subsequent analysis.

2.2. Analytical methods

2.2.1. Metabolite extraction from tissue samples

Each frozen tissue was taken from the container, weighted (50–100 mg) and placed into a 2-mL cryovial containing approximately 100 mg of a mixture of zirconia oxide beads with diameters of 0.7, 1.4 and 2.8 mm at a proportion ratio 1:1:1 (Bertin Corp., Rockville, MD, USA). A total of 500 μL of cold acetonitrile (Optima LCMS grade, Fisher, Leicester, UK) was added to the cryovial and homogenized in a bead beater (Precellys, Bertin Corp, Rockville, MD, USA) with three cycles at 6500 rpm for 20 s per cycle. The residual homogenized sample in acetonitrile (approximately 400 μL) was centrifuged at 17,949 *g* for 15 min at 4°C (Eppendorf 5430 R Centrifuge, Hamburg Germany). The tissue extract supernatant was transferred and stored at −80°C in 1.5 mL microcentrifuge tubes until derivatization step.

2.2.2. Plasma sample extraction

Samples were thawed at room temperature and briefly vortexed. A total of 25 μL plasma was transferred into a 1.5 mL microcentrifuge tube (Eppendorf, Hamburg, Germany) containing 50 μL cold acetonitrile (LCMS Optima grade, Fisher, Leicester, UK) and mixed for a few seconds. The tube was centrifuged for 15 min at 17,949 *g* at 4°C (Eppendorf 5430 R Centrifuge, Hamburg Germany) and stored at −80°C until derivatization.

2.2.3. Preparation of standards and labelled internal standards

TMA 40 % solution (Sigma-Aldrich, Steinheim, Germany) and TMA-*N*-oxide•$2H_2O$ with 98–99 % purity (Fluka, Charlotte, NC, USA) were used to prepare standard stock solutions and serial calibration curves as detailed in supplementary table (Tables S1 and S2). TMA-D_9-hydrochloride (Cayman. Ann Harbor, MI, USA) and TMA-D_9-*N*-oxide (Toronto Research Chemicals, North York, Ontario, Canada) were prepared in acetonitrile (Optima LCMS grade, Fisher, Leicester, UK) at 160 μM and 50 μM, respectively, as labelled internal standards and stored at −20°C in silanized glass vials (Table S3).

2.2.4. Derivatization and ion pairing reactions

Derivatization using ethyl bromoacetate (EBA) was considered as one of the best options to obtain mass differentiation between the two analytes and has been successfully applied previously [9,14]. An aliquot of 10 μL of sample extracts or prepared standard solution was transferred into a 1.5 mL microcentrifuge tube, which contained 10 μL internal standard solution mixture prepared as described above and 45 μL of EBA (Sigma-Aldrich, Steinheim, Germany) solution (15 mg/mL, 1 % v/v ammonium hydroxide in acetonitrile). The samples were thoroughly mixed and incubated at room temperature for 30 min. In this derivatization process, TMA was derivatized, but TMAO remained in its original form due to the oxygen present in the structure. Subsequently, 185 μL of a cold solution consisting of 95 % acetonitrile and 5 % water (v/v) was added to the tubes to quench the reaction. Following thorough mixing, the tubes were centrifuged at 17,949 *g* for 10 min. A fraction of 100 μL of the supernatant was transferred to a 300-μL injection vial with a conical bottom (Part No. WAT094172, Waters™), followed by adding 50 μL 1 M sodium heptanesulphonate (ion pairing reagent) prepared in water (Sigma-Aldrich, Steinheim, Germany), mixing well and storing at 4°C until injection (Fig. 1).

2.2.5. UPLC-MS/MS

Chromatographic separation was performed on a Waters Acquity Binary Management UHPLC system (Milford, CT, USA) on a Waters HSS T3 C18 Column with dimensions 150 mm × 2.1 mm, 1.8 μm pore size. Mobile phase A (MPA) was water (Optima LCMS Grade, Fisher, Leicester, UK) containing 0.1 % formic acid (Supelco, Bellefonte, PA, USA). Mobile phase B (MPB) was acetonitrile (Optima LCMS grade, Fisher, Leicester, UK) with 0.1 % formic acid. Chromatographic separation is described in Table S4. Column temperature was kept constant throughout separation at 40°C, flow rate at 0.35 mL/min, injection loop volume of 2 μL and total running time of 6 min. TMA and TMAO were eluted at 2.51 min, their deuterated counterparts at 2.50 min, and derivatized TMA (146>118) and TMA-d_9 (155>127) at 2.7 min (Table 2). All transitions were detected in positive electrospray ionization polarity (ESI+) on a Waters Xevo TQ-S (Waters, Milford, CT, USA). Source and desolvation temperatures were set to 150ºC and 500ºC, respectively. Desolvation gas flow was 800 L/hr and capillary voltage was 1 KV. Cone and collision energy voltages are shown in Table 2. Calculation of concentrations are described in the Supplementary Information.

2.3. Statistical analyses

GraphPad Prim 9.0 (GraphPad Prism version 9.0.0 for Windows, GraphPad Software, San Diego, CA, USA) was used for analysis of means (2 sample t-tests) and Wilcoxon tests reported with 95 % confidence limits. Mean results were presented with standard error of the mean (s.e.m) in box plots and tables. Linear regression equations from standard calibration curves, r-square, accuracy and precision values with coefficient of variation percentages (relative standard deviation) and standard errors of the mean were calculated in Excel 365 (Microsoft 365, Microsoft Corporation, Version 16.0).

3. Results and discussion

3.1. Optimization of UPLC-MS method

TMA and TMAO are challenging to be retained and detected by a conventional chromatographic system due to their small molecular

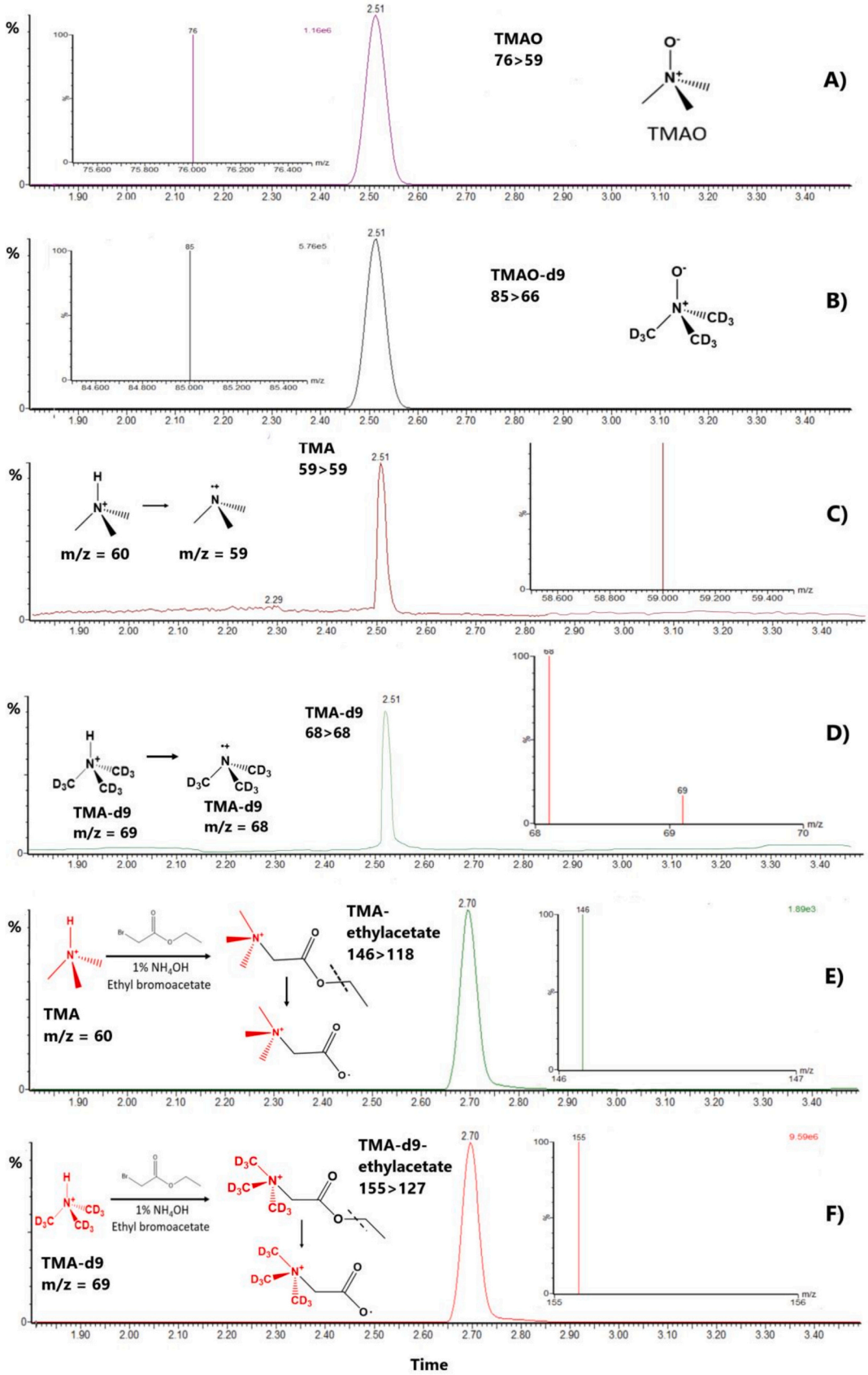

Fig. 2. Chromatograms and mass spectra for a solution containing: A) 50 μmol/L TMAO; B) 50 μmol/L TMAO-d_9; C) non-derivatized TMA; D) non-derivatized TMA-d_9; E) 50 μmol/L derivatised TMA; and F) 50 μmol/L derivatised TMA-d_9. X axis is retention time in minutes.

weight, polarity, and different physical properties. For example, boiling point for TMA is 2.9°C, whereas TMAO is at 158°C. Owing to low boiling point of TMA, we observed lower response signals of both TMA and TMA-d_9 in solutions stored at 4°C overnight compared to those in the freshly prepared solution. Therefore, solutions used in the current study were stored at −20°C. To obtain a fast and reliable method to separate these amines, we first tested several chromatographic methods including HILIC and reverse phase (RP). When separating a solution that contained 25 μM TMA, 160 μM TMA-d_9, 25 μM TMAO and 50 μM TMAO-d_9, a HILIC BEH 2.1 ×150 mm column (Waters, Milford, USA) separation presented much lower peak intensity (6.1 $\times 10^4$) and broad peak shape compared to RP columns, such as C18 HSS T3 2.1 ×150 mm (Waters, Milford, USA) shown in Figures S1 A&B.

Subsequently, we incorporated an ion pairing solution containing 1 M sodium heptanesulfonate (SHS) into the samples to increase the retention of polar amines. SHS has been reported for improving retention of ionisable structured compounds including amino acids and pharmaceuticals in positive mode [19,20]. The use of the ion pairing reagent allows to form an anionic counter-ion donor to the protonated TMA and TMAO ($R–NH_3^+ + CH_3(CH_2)_6–SO_3^- \rightarrow R–NH_3^+ \ ^-O_3S–(CH_2)_6CH_3$) and increases hydrophobicity and retention. The effectiveness of ion-pairing depends firstly on the adjustment of the pH to 9.5 in the sample rather than incorporating it to the mobile phase, and secondly, by maintaining the sample to SHS volume ratio (2:1) constant. We tested the sample with two RP C18 columns. The C18 HSS T3 column produced a better peak shape with a higher intensity of TMA signal compared to the CSH C18 2.1 ×100 mm (Waters, Milford, USA) column (Figs S1 C&D). Therefore, we opted to use the C18 HSS T3 column for the subsequent analyses.

3.2. Selection of ions for TMA and TMAO quantification

One of the main capabilities of a triple quadrupole (TQ) is its sensitivity and selectivity. In the case of TMAO ($m/z = 76$) and TMAO-d_9 ($m/z = 85$), we obtained multiple reaction monitoring (MRM) as 76 > 59 and 85>66, respectively (Figs. 2A and 2B, Table 2), which corresponded to values previously reported in other studies as the main transitions in positive (ESI^+) mode [7,21,22].

However, for TMA, with 59 amu, further fragmentation was not possible in our instrument, due to the detection mass range starting from 50 to 1000 amu at a rate of 10 scans per second. We observed that ionization for TMA formed a protonated ion at $m/z = 60$ ($C_3H_9N + H$), but its signal was small compared to $m/z = 59$ ($C_3H_9N^+$) (Fig. 2C). Similarly, we observed another peak for $m/z = 58$ ($C_3H_8N^+$), which also presented a much smaller signal compared to $m/z = 59$. Although, other studies reported ion transitions at 60 > 44 [18] and 60 > 45 [15,18], we did not detect these fragment signals nor strong signals at $m/z = 60$. Furthermore, intensities of the response for 59>58 transition was very low and not ideal for use of metabolite quantitation. Therefore, we selected ion pairs at 59 > 59 and 68>68 for quantifying TMA and TMA-d_9, respectively (Fig. 2C & 2D).

Furthermore, signals of 59>59 with low intensities in blank samples were noted (Fig. S2A) and it is unlikely to be the residual TMA from previously injected samples since blanks injected prior to standard calibration curve samples also contained this peak. While we are not certain about its sources, it is possible that the reaction of acetonitrile and ammonium (from ammonium hydroxide added to the samples to adjust pH) during ionization formed a peak at $m/z = 59$ ($(CH_3CN{+}NH_4)^+$) in ESI^+ mode, which could elute at the same time to the analytes (co-elution) and contributed to the background signal. Additionally, we observed TMA signals of 59 > 59 when injecting pure solutions of TMAO and TMAO-d_9 (Fig. S2B). Collectively, these observations indicate that contributions from various unknown sources to signal 59>59 intensities could bias the quantification of TMA.

Since TMAO and TMA commonly co-exist in biological samples in addition to other important key metabolites that share the same nominal mass as TMA (such as *N*-methyl formamide, acetaldehyde oxime, acetamide and 2-aminoacetaldehyde), we incorporated a derivatization step into the sample preparation, allowing us to accurately quantitate both compounds, minimizing interferences of these unknown sources on TMA quantification.

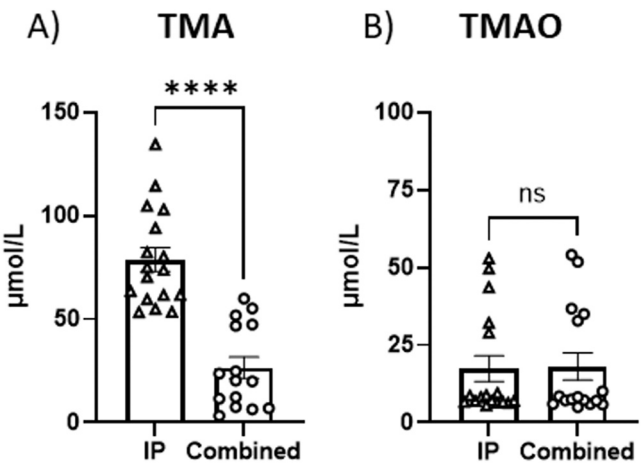

Fig. 3. Measured concentrations of TMA (A) and TMAO (B) in mouse plasma using ion pairing (IP) alone or combination of IP and derivatization with ethyl bromoacetate (combined). Wilcoxon matched pairs test. **** indicate $p < 0.001$; ns: not statistically significant. Data presented as mean ± s.e.m.

TMAO was not derivatised due to the oxygen present in the structure. Derivatized TMA-d_9 as TMA-d_9-ethyl-acetate and TMA as TMA-ethyl-acetate were detected at 2.70 min with ion transitions of 155>127 (Fig. 2E) and 146>118 (Fig. 2F), respectively. With the introduction of derivatization, we selectively separated TMA and TMAO from other metabolites abundantly present in plasma, avoiding potentially biased compounds with similar masses. In our experiments, the derivatization rate of TMA-d_9 was 99 % and for TMA was 97 %, suggesting an efficient TMA derivatization process. The results showed that the combination of ion pairing and EBA derivatization reduced these interferences on the quantification of TMA in plasma compared to using ion pairing alone (Fig. 3A), while ion pairing or this combined method showed very similar TMAO quantification (Wilcoxon matched pairs test, $p = 0.9$) (Fig. 3B).

3.3. Assessment of the quantification method

The combined method (EBA-ion pairing) was assessed by calculating response ratios of pure standard calibrators against labeled internal standards to compensate for matrix effects as recommended by the Food and Drug Administration (FDA) for clinical validation [23]. We pooled 10 μL plasma samples from 10 mice and diluting it with deionized water by ten-fold. Ten-point calibration curves were generated based on the peak area ratios of the pure analytes and internal standards (without weight factor) for three consecutive days (2 calibration curves per day), as well as monitoring quality control samples (the pooled plasma) spiked with TMA and TMAO at 5 μM, 50 μM and 100 μM. Results from calibration curves showed great linearity for TMA ($R^2 > 0.993$, n = 6) and TMAO ($R^2 > 0.996$, n = 6). Lower limits of detection (LOD) for both analytes were established at signal to noise ratio ≥ 10; and lower limit of quantitation (LLOQ) was calculated as LOD*3. The detection ranges were from 0.1 μM to 300 μM for TMA and from 0.01 μM to 300 μM for TMAO. In addition, LLOQ was evaluated from triplicate measurements of solution mixtures containing TMA and TMAO and the chromatograms are shown in Figure S3A. Coefficients of variations were <15 % for TMA at 0.1 μmol/L (n = 3) and 0.01 μmol/L for TMAO (n = 3) indicating higher sensitivity for TMAO compared to TMA. Quality control samples were assessed in triplicate to obtain intra (n=2) and inter-day precision

Table 3
Inter- and intra-day precision and accuracy of quality control samples for method validation.

		TMA Inter-day (n = 6)					TMAO Inter-day (n = 6)				
	Nominal concentration	Observed concentration			Precision	Accuracy	Observed concentration			Precision	Accuracy
QC	µM	µM		s.e.m	%	%	µM		s.e.m	%	%
Low	5	5.18	±	0.03	5.78	103.62	5.52	±	0.01	1.91	110.37
Medium	10	10.73	±	0.01	0.96	107.31	11.19	±	0.04	3.55	111.92
High	50	58.10	±	0.14	2.08	116.21	54.96	±	0.29	4.73	109.93
		TMA Intra-day (n = 2)					**TMAO Intra-day (n = 2)**				
	Nominal concentration	Observed concentration			Precision	Accuracy	Observed concentration			Precision	Accuracy
QC	µM	µM		s.e.m	%	%	µM		s.e.m	%	%
Low	5	5.03	±	0.00	0.15	100.65	5.67	±	0.02	1.74	113.30
Medium	10	10.18	±	0.08	3.19	101.79	11.39	±	0.06	1.96	113.86
High	50	56.15	±	0.40	2.83	112.30	55.14	±	0.80	5.79	110.27

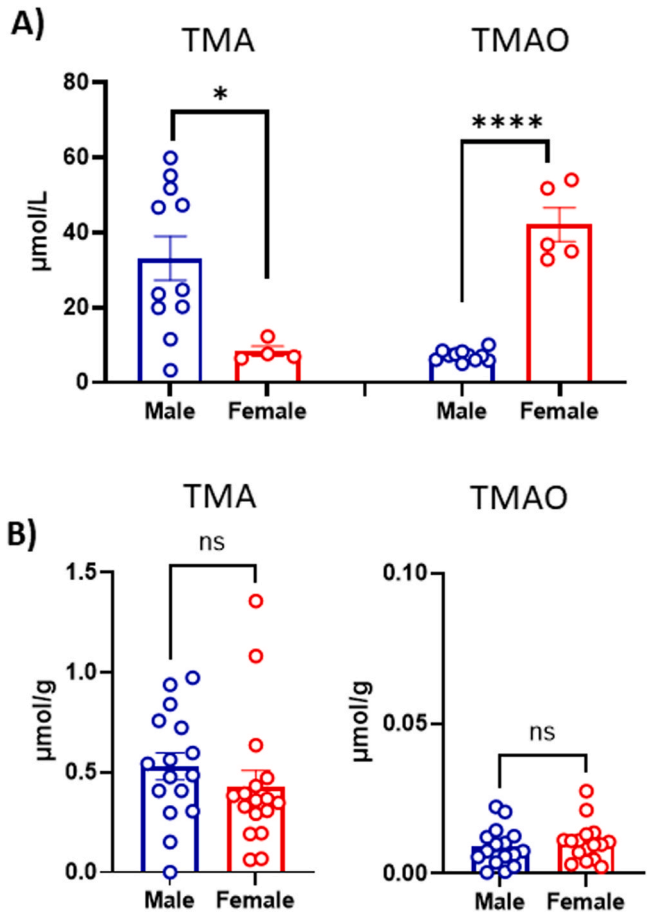

Fig. 4. Measurement of TMA and TMAO concentrations in (A) plasma and (B) colonic tissue extracts of male and female mice using the combined method of derivatisation with EBA and ion-pairing. Mann Whitney test. * $p<0.05$; **** $p<0.001$; ns, not statistically significant. Data are presented as mean ± s.e.m.

values in three consecutive days (n=6) with 0.96 – 4.73 % for inter-day, and 0.15–5.79 % for intra-day precision (Table 3). Inter-day accuracy values ranged from 3.62 % to 16.21 % and intra-day accuracy from 0.65 % to 13.86 % (Table 3). Carry over effects were monitored for both TMAO and TMA by comparing their peak areas against a blank sample (sample that did not contain analyte or internal standards) injected after the largest calibration standard at 300 µM. The peaks for both compounds were below 1 % to the peak area obtained for the largest calibrator at 300 µM. The sensitivity, accuracy and precision values suggest a robust and repeatable method capable to quantitate TMA and TMAO in biological samples.

3.4. Quantification of TMA and TMAO in plasma and colonic extracts

TMA and TMAO concentrations were quantified using the combined method in plasma and colonic tissue obtained from male and female mice. Plasma TMA in males (n= 11) mean value was significantly higher ($p = 0.027$) at 33.1 ± 5.9 µmol/L compared to females (n = 4) at 8.3 ± 1.39 µmol/L (Fig. 4A). In contrast, TMAO concentrations were significantly ($p < 0.0001$) lower in male (7.2 ± 0.4 µmol/L) compared to females (42.1 ± 4.5 µmol/L) (Fig. 4A). The chromatograms of plasma and colonic tissue are shown in Figures S3B and S3C. These results agree with previously reported levels of TMA and TMAO in mice [24,25]. The higher level of TMAO in female mice is likely owing to higher expression levels of flavin monooxygenases (FMOs), which convert TMA to TMAO in the liver in female than in male mice, and male mice suppress TMAO formation in the liver due to the presence of sex steroids [24].

We measured TMA and TMAO concentrations in the colon tissue and found no statistically significant difference (Mann Whitney test $p = 0.17$) between male (n = 16) at 0.53 ± 0.1 µmol/g and female mice (n=16) at 0.45 ± 0.1 µmol/g (Fig. 4B). Similarly, there were no statistically significant differences (Mann Whitney test, $p = 0.468$) in TMAO levels between male (n = 16) at 8.9 ± 1.6 nmol/g, and female (n = 16) mice at 10.6 ± 1.6 nmol/g (Fig. 4B).

4. Conclusions

This study demonstrated that the caution should be paid to the potential interferences of other compounds on TMA quantification. We reported that a combined method, applying both derivatization with EBA and an ion-pairing reagent, yielded superior results in terms of TMA and TMAO quantification in biological samples with high accuracy and precision. This method will facilitate further biological investigations on these compounds.

CRediT authorship contribution statement

Jia Li: Writing – review & editing, Supervision, Resources, Funding acquisition, Conceptualization. **Yang Bi:** Writing – review & editing, Investigation. **Maria A. Valdivia-Garcia:** Writing – review & editing, Writing – original draft, Visualization, Validation, Methodology, Investigation, Formal analysis, Data curation, Conceptualization. **Kaoutar Abaakil:** Writing – review & editing, Investigation.

Author contributions

JVL obtained funding for the project. LC-MS method experiments and sample extraction were conducted by MAVG. Mice tissue dissections were conducted by YB and KA. The manuscript was drafted by MAVG and reviewed by all authors.

Funding

This work was fully funded by The European Research Council (ERC) Starting Grant (715662).

Declaration of Competing Interest

The authors declare the following financial interests/personal relationships which may be considered as potential competing interests: Jia Li reports financial support was provided by Imperial College London. Jia Li reports a relationship with Cardiff University that includes: consulting or advisory. Jia Li reports a relationship with Khon Kaen University that includes: travel reimbursement. If there are other authors, they declare that they have no known competing financial interests or personal relationships that could have appeared to influence the work reported in this paper.

Data availability

Data will be made available on request.

Acknowledgments

This work was fully funded by the European Research Council (ERC) Starting Grant (715662) and Chinese Scholarship Council for supporting PhD studies of Yang Bi. All LC-MS analysis was carried out at the National Phenome Center at Imperial College London.

Appendix A. Supporting information

Supplementary data associated with this article can be found in the online version at doi:10.1016/j.jpba.2024.116480.

References

[1] R.L. Loo, Q. Chan, J.K. Nicholson, E. Holmes, Balancing the equation: a natural history of trimethylamine and trimethylamine-N-oxide, J. Proteome Res. 21 (3) (2022) 560–589.
[2] G.G. Schiattarella, A. Sannino, E. Toscano, G. Giugliano, G. Gargiulo, A. Franzone, B. Trimarco, G. Esposito, C. Perrino, Gut microbe-generated metabolite trimethylamine-*N*-oxide as cardiovascular risk biomarker: a systematic review and dose-response meta-analysis, Eur. Heart J. 38 (39) (2017) 2948–2956.
[3] P. Andrikopoulos, J. Aron-Wisnewsky, R. Chakaroun, A. Myridakis, S.K. Forslund, T. Nielsen, et al., Evidence of a causal and modifiable relationship between kidney function and circulating trimethylamine *N*-oxide, Nat. Commun. 14 (1) (2023) 5843.
[4] H. Zou, C. Huang, L. Zhou, R. Lu, Y. Zhang, D. Lin, NMR-based metabolomic analysis for the effects of trimethylamine N-oxide treatment on C2C12 myoblasts under oxidative stress, Biomolecules 12 (9) (2022).
[5] K.J. Burton, R. Kruger, V. Scherz, L.H. Munger, G. Picone, N. Vionnet, et al., Trimethylamine-*N*-oxide postprandial response in plasma and urine is lower after fermented compared to non-fermented dairy consumption in healthy adults, Nutrients 12 (1) (2020).
[6] J. Fiori, S. Turroni, M. Candela, P. Brigidi, R. Gotti, Simultaneous HS-SPME GC-MS determination of short chain fatty acids, trimethylamine and trimethylamine *N*-oxide for gut microbiota metabolic profile, Talanta 189 (2018) 573–578.
[7] L.M. Heaney, D.J. Jones, R.J. Mbasu, L.L. Ng, T. Suzuki, High mass accuracy assay for trimethylamine *N*-oxide using stable-isotope dilution with liquid chromatography coupled to orthogonal acceleration time of flight mass spectrometry with multiple reaction monitoring, Anal. Bioanal. Chem. 408 (3) (2016) 797–804.
[8] K.A. daCosta, J.J. Vrbanac, S.H. Zeisel, The measurement of dimethylamine, trimethylamine, and trimethylamine N-oxide using capillary gas chromatography-mass spectrometry, Anal. Biochem. 187 (2) (1990) 234–239.
[9] M.E. Hefni, M. Bergstrom, T. Lennqvist, C. Fagerstrom, C.M. Witthoft, Simultaneous quantification of trimethylamine *N*-oxide, trimethylamine, choline, betaine, creatinine, and propionyl-, acetyl-, and L-carnitine in clinical and food samples using HILIC-LC-MS, Anal. Bioanal. Chem. 413 (21) (2021) 5349–5360.
[10] H.M. Awwad, J. Geisel, R. Obeid, Determination of trimethylamine, trimethylamine *N*-oxide, and taurine in human plasma and urine by UHPLC-MS/MS technique, J. Chromatogr. B Anal. Technol. Biomed. Life Sci. 1038 (2016) 12–18.
[11] E.C. Robanus-Maandag, P.J. Koelink, C. Breukel, D.C. Salvatori, S.C. Jagmohan-Changur, C.A. Bosch, H.W. Verspaget, P. Devilee, R. Fodde, R. Smits, A new conditional Apc-mutant mouse model for colorectal cancer, Carcinogenesis 31 (5) (2010) 946–952.
[12] B.N. Zordoky, M.M. Sung, J. Ezekowitz, R. Mandal, B. Han, T.C. Bjorndahl, et al., Metabolomic fingerprint of heart failure with preserved ejection fraction, PLOS ONE 10 (5) (2015) e0124844.
[13] M.A. Bain, R. Faull, G. Fornasini, R.W. Milne, A.M. Evans, Accumulation of trimethylamine and trimethylamine- N -oxide in end-stage renal disease patients undergoing haemodialysis, Nephrol. Dial. Transplant. 21 (5) (2006) 1300–1304.
[14] D.W. Johnson, A flow injection electrospray ionization tandem mass spectrometric method for the simultaneous measurement of trimethylamine and trimethylamine N-oxide in urine, J. Mass Spectrom. 43 (4) (2008) 495–499.
[15] T. Roggensack, B. Merz, N. Dick, A. Bub, R. Kruger, Targeted ultra-performance liquid chromatography/tandem mass spectrometric quantification of methylated amines and selected amino acids in biofluids, Rapid Commun. Mass Spectrom. 34 (7) (2020) e8646.
[16] S. Veeravalli, K. Karu, I.R. Phillips, E.A. Shephard, A highly sensitive liquid chromatography electrospray ionization mass spectrometry method for quantification of TMA, TMAO and creatinine in mouse urine, MethodsX 4 (2017) 310–319.
[17] L. Hoyles, M.L. Jiménez-Pranteda, J. Chilloux, F. Brial, A. Myridakis, T. Aranias, C. Magnan, G.R. Gibson, J.D. Sanderson, J.K. Nicholson, D. Gauguier, A. L. McCartney, M.E. Dumas, Metabolic retroconversion of trimethylamine N-oxide and the gut microbiota, Microbiome 6 (1) (2018) 73.
[18] Y.Y. Cai, F.Q. Huang, X. Lao, Y. Lu, X. Gao, R.N. Alolga, et al., Integrated metagenomics identifies a crucial role for trimethylamine-producing Lachnoclostridium in promoting atherosclerosis, npj Biofilms Microbiomes 8 (1) (2022) 11.
[19] G. Andraws, S. Trefi, Ionisable substances chromatography: a new approach for the determination of Ketoprofen, Etoricoxib, and Diclofenac sodium in pharmaceuticals using ion - pair HPLC, Heliyon 6 (8) (2020) e04613.
[20] S. Moldoveanu, V. David, Chapter 10 - Other HPLC separations performed on hydrophobic stationary phases, in: S. Moldoveanu, V. David (Eds.), Essentials in Modern HPLC Separations (Second Edition), Elsevier, 2022, pp. 421–446.
[21] D. Bhandari, B.A. Bowman, A.B. Patel, D.M. Chambers, V.R. De Jesus, B.C. Blount, UPLC-ESI-MS/MS method for the quantitative measurement of aliphatic diamines, trimethylamine N-oxide, and beta-methylamino-l-alanine in human urine, J. Chromatogr. B Anal. Technol. Biomed. Life Sci. 1083 (2018) 86–92.
[22] W. Yu, C. Xu, G. Li, W. Hong, Z. Zhou, C. Xiao, et al., Simultaneous determination of trimethylamine N-oxide, choline, betaine by UPLC-MS/MS in human plasma: An application in acute stroke patients, J. Pharm. Biomed. Anal. 152 (2018) 179–187.
[23] U.S. Department of Health and Human Services Food and Drug Administration, Center for Biologics Evaluation and Research (CBER) Analytical Procedures and Methods Validation for Drugs and Biologics Guidance for Industry in: C.f.D.E.a.R.C. U.S. Department of Health and Human Services Food and Drug Administration, Center for Biologics Evaluation and Research (CBER) (Ed.) Pharmaceutical Quality/CMC, FDA Goverment, New Hampshire, Maryland, 2015, p. 18
[24] Y. Hasegawa, S.Y. Chen, L. Sheng, P.K. Jena, K.M. Kalanetra, D.A. Mills, Y.Y. Wan, C.M. Slupsky, Long-term effects of western diet consumption in male and female mice, Sci. Rep. 10 (1) (2020) 14686.
[25] C.L. Gavaghan McKee, I.D. Wilson, J.K. Nicholson, Metabolic phenotyping of nude and normal (Alpk:ApfCD, C57BL10J) mice, J. Proteome Res. 5 (2) (2006) 378–384.